Analysis of Nonlinear Stress-Strain Behavior of Fiber-Reinforced Composite Materials

Robert M. Jones* and Harold S. Morgan†
Southern Methodist University, Dallas, Texas

Fiber-reinforced composite materials generally exhibit nonlinear stress-strain behavior in at least one of the principal material directions. For example, boron/epoxy and graphite/epoxy have highly nonlinear shear behavior. Moreover, boron/aluminum has nonlinear behavior transverse to the fibers as well as a shear nonlinearity, and carbon/carbon has nonlinearities in all principal material directions. The Jones-Nelson strain energy based nonlinear mechanical property model is extended to treat all nonlinearities of fiber-reinforced composites. The basic model will converge only up to a specific strain energy value. That limitation is eased by using new extrapolations of the stress-strain curve and mechanical property - energy curve for strain energies above available stress-strain data. These extrapolations are necessary because the strain energies of biaxial loading exceed the strain energies of uniaxial loading under which the properties are defined and because the maximum strain energies under uniaxial loading are different in the various principal directions due to orthotropy. Strains predicted with the new material model correlate well with strains measured by Cole and Pipes in uniaxial off-axis loading of boron/epoxy and graphite/epoxy. The predicted strains are also close to strains predicted by Hahn and Tsai, who use a material model with a single (shear) nonlinearity. Our model can be used for the several nonlinearities of boron/aluminum and carbon/carbon; therefore, it is more widely applicable than the Hahn and Tsai model.

Nomenclature

A_i, B_i, C_i, U_{0i}	= constants in ith mechanical property equation [Eq. (1)]
E_1	= Young's modulus in the 1 direction of a lamina
E_2	= Young's modulus in the 2 direction of a lamina
G_{12}	= shearing modulus in the 1-2 plane of a lamina
U	= strain energy function [Eq. (2)]
γ_{12}	= shearing strain in 1-2 plane
ϵ_1, ϵ_2	= normal strains in principal material directions
θ	= angle of orientation of off-axis loading tests
ν_{12}	= Poisson's ratio for contraction (expansion) in the 2 direction due to tension (compression) in the 1 direction
σ_1, σ_2	= normal stresses in principal material directions
$\sigma_x (\epsilon_x)$	= normal stress (strain) in x direction at angle θ to 1 direction
Subscript	
sec	= secant modulus

Introduction

THE linear elastic theory of fiber-reinforced composite materials is well developed (see, for example, Jones[1]). However, most composite materials exhibit nonlinear stress-strain behavior in at least one of the principal material directions. For example, the stress-strain curve in the fiber (1) direction of a unidirectionally reinforced lamina is linear in Fig. 1, even at high stress levels. However, the stress-strain response in the 2 direction transverse to the fibers is often somewhat nonlinear. Moreover, the shear response is quite nonlinear in Fig. 1. The degree of nonlinearity varies from composite to composite and is due mainly to the nonlinear matrix material, which greatly affects the transverse modulus E_2 and the shear modulus G_{12} of the composite. The effect of the nonlinear matrix material on the longitudinal modulus E_1 and Poisson's ratio ν_{12} is shown with micromechanics analysis to be negligible for normal combinations of fibers and matrix materials.[1]

Specific examples of fiber-reinforced composite materials with nonlinear stress-strain behavior include boron/epoxy and graphite/epoxy with a slight E_2 nonlinearity (that is usually ignored), but a strong G_{12} nonlinearity.[2] On the other hand, metal-matrix composites such as boron/aluminum have strong E_2 and G_{12} nonlinearities.[3] Three-dimensionally fiber-reinforced composites such as carbon/carbon have nonlinearities in all principal material directions.[4] The nonlinearities for all of these materials are more pronounced with increasing temperature and, for the epoxy-based composites, with increasing moisture content (since the resinous matrix material absorbs moisture).[5] Thus, general application of composites requires analysis of nonlinear stress-strain behavior.

Various investigators have attempted to include mechanical property nonlinearities in analysis of composite materials.[6-13] Petit and Waddoups[6] use an incremental approach to

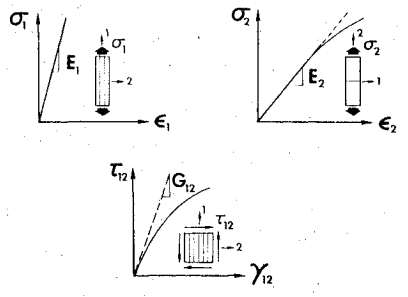

Fig. 1 Typical stress-strain curve behavior of fiber-reinforced composite materials.

Presented at the 17th AIAA/ASME/SAE Structures, Structural Dynamics, and Materials Conference, Valley Forge, Pa., May 5-7, 1976 (in bound volume of Conference Papers, no paper number); submitted May 28, 1976; revision received July 5, 1977.

Index categories: Structural Composite Materials; Structural Statics; Materials, Properties of.

*Professor of Solid Mechanics. Associate Fellow AIAA.

†Research Assistant; now Member of the Technical Staff, Missile and Ordnance Division, Texas Instruments, Inc., Dallas, Texas.

determine the stress-strain response of a lamina. Hashin, Bagchi, and Rosen[7] use Ramberg-Osgood stress-strain relations to approximate the nonlinearities. Hahn and Tsai[8] model the nonlinear shear behavior of boron/epoxy and graphite/epoxy and regard all other stress-strain curves as linear. Their predictions of strain response under uniaxial off-axis loading (i.e., loading in other than principal material directions) agree fairly well with measurements by Cole and Pipes.[2] Sandhu[9] fits a spline approximation to the shear behavior and gets closer agreement with Cole and Pipes' data than do Hahn and Tsai.

Jones and Nelson[10-13] develop an orthotropic material model in which the nonlinear mechanical properties are functions of the strain energy density,

$$\text{mechanical property}_i = A_i[1 - B_i(U/U_{0_i})^{C_i}] \quad (1)$$

where

$$U = (\sigma_1\epsilon_1 + \sigma_2\epsilon_2 + \tau_{12}\gamma_{12})/2 \quad (2)$$

for a lamina under plane stress and A_i, B_i, and C_i are the initial slope, initial curvature, and change of curvature of the ith stress-strain curve. The quantity U_0 is used to nondimensionalize the strain energy portion of the mechanical property equation. The Jones-Nelson model is used in an iteration procedure which converges to the state of stress and strain with a secant modulus corresponding to an equivalent linear elastic body. The number of nonlinear properties is not restricted; i.e., all properties or only a select few can be nonlinear. Also, under multiaxial loading, the nonlinear properties are determined by using all stresses of the multiaxial stress state through the strain energy density. Thus, the values of the mechanical properties do not change under rotation of coordinates. Jones and Nelson accurately predict the behavior of ATJ-S graphite under uniaxial and biaxial loading.[10-13] ATJ-S graphite is a granular or particulate composite material with low orthotropy ($E_1/E_2 = 1.3$) in contrast to highly orthotropic fiber-reinforced composite materials.

We use in the foregoing the term "material model," which also might be used to refer to the stress-strain relations. However, we interpret the material model to be the set of mechanical property vs energy equations plus the associated iteration procedure. The steps necessary to define and verify the material model for a particular material are: 1) fit the mechanical property equations to uniaxial stress-strain data in principal material directions to define the basic material model; 2) use the material model to predict strains measured under uniaxial loading in other than principal material directions; and 3) use the material model to predict strains measured under biaxial loading (in principal material directions and in other than principal material directions). If the predicted and measured strains agree well in the foregoing steps, then the material model is regarded as validated. However, measurements available for specific materials are often not sufficient for the preceding comparisons to be made. Thus, most material models are not validated as well as we would like them to be.

All previous attempts to analyze nonlinear stress-strain behavior of fiber-reinforced composite materials are limited in some way. Petiti and Waddoups[6] and Hashin, Bagchi, and Rosen[7] do not determine the mechanical properties in multiaxial stress states by use of all the stresses (σ_1, σ_2, and τ_{12}); i.e., the multiaxial nonlinear stress-strain behavior is uncoupled into a series of uniaxial models. Hahn and Tsai[8] can handle only materials with a single nonlinearity (in shear). Sandhu[9] uses an approximation of the stress-strain behavior under biaxial normal stress states to predict equivalent multiaxial strain increments in his incremental theory. In contrast, mechanical properties can be nonlinear in all principal material directions in the Jones-Nelson model[10-13] and are determined from the multiaxial stress state through use of the strain energy concept in a computationally simpler and physically more attractive manner. However, the Jones-Nelson model has not been applied to fiber-reinforced composite materials.

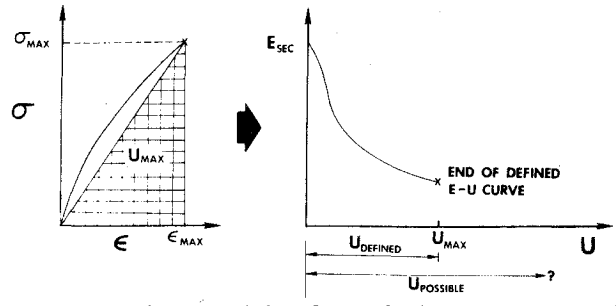

Fig. 2 Limit of measured data for mechanical property vs strain energy curve.

The objective in this paper is to extend and adapt the Jones-Nelson nonlinear material model to fiber-reinforced composite materials. The key elements of the extension are the treatment of stronger nonlinearities along with more highly orthotropic behavior than for the graphitic material for which the model was developed. In the process of extending the model, we identify a limiting value of strain energy beyond which the model iteration procedure will not converge. This value corresponds to the top of the hump in the implied stress-strain curve. Accordingly, we must extend the mechanical property - energy behavior or alternatively the stress-strain behavior so that a hump in the stress-strain behavior never exists. How we perform this extension is discussed in "Material Model Extensions." Then, we use the Jones-Nelson model and the new model to predict strains under uniaxial off-axis loading (i.e., in other than principal material directions) or boron/epoxy and graphite/epoxy laminae. We compare our predicted strains both with Cole and Pipes' measured strains and with Hahn and Tsai's predicted strains. No uniaxial off-axis strain measurements are known for boron/aluminum. Thus, the full capability of the new model cannot be assesed quantitatively. That assessment will be made when sufficient data are available.

Material Model Extensions

Motivation for Extensions

The basic Jones-Nelson material model is applicable only over the range in which data are defined. That is, a maximum strain energy U_{max} as the limit of the defined data exists for each mechanical property as in Fig. 2. However, the actual strain energy can exceed the defined range of mechanical property vs strain energy curves for two reasons. First, the nonlinear model is applied in multiaxial stress states for which the strain energy is higher than in the uniaxial stress states in which the mechanical properties are measured. All stresses and strains of a multiaxial stress state contribute to the value of U; thus, the multiaxial strain energy can be shown to be up to 50% bigger than the strain energy in a uniaxial stress state.

The second reason for existence of strain energies above the defined range is that orthotropic materials have drastically different stiffnesses and load capacities, and hence drastically different strain energy capacities, in different directions. The strain energy capacities for loading in the 2 direction and for shear loading are generally much lower than for loading in the 1 direction. For example, a material might have U_{max} of 250 psi for the $\sigma_1 - \epsilon_1$ curve but only 50 psi for the $\sigma_2 - \epsilon_2$ curve. However, these uniaxial strain energy capacities are not the capacities of the material under multiaxial loading. Nor are they the capacities of the material under off-axis uniaxial loading for which the maximum strain energy can be much larger than the U_{max} for which $E_{2_{sec}}$ is defined. Accordingly, we must find a way of rationally extending the uniaxial stress-

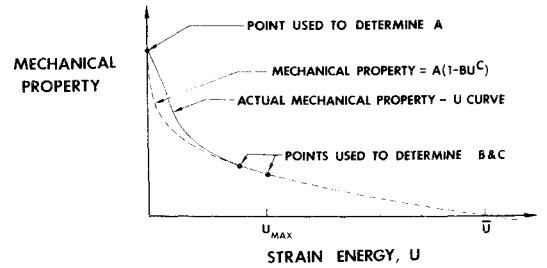

Fig. 3 Actual vs extended approximate mechanical property vs strain energy behavior.

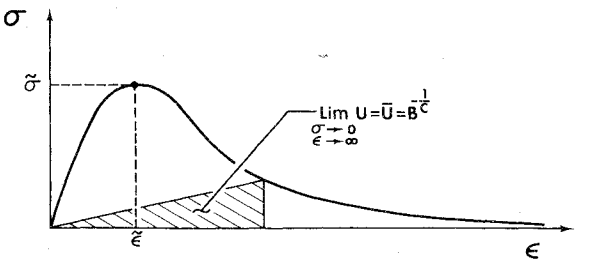

Fig. 4 Representative Jones-Nelson model implied stress-strain curve.

strain and mechanical property vs strain energy information to multiaxial stress states.

In what follows, we first arbitrarily extend the basic Jones-Nelson material model past the defined data and determine the consequences and implications of such an extension. Then, we develop a new extrapolation of the stress-strain curve suitable for fiber-reinforced composite materials.

Extension of Jones-Nelson Material Model

The simplest way to extrapolate the mechanical property vs strain energy curve is to use the mechanical property equation, Eq. (1), for values of U beyond the defined range of strain energy in Fig. 2. The representative mechanical property vs strain energy curve in Fig. 3 is defined for strain energies up to U_{max}; hence, the solid curve is used to designate the actual data. The dashed curve in Fig. 3 is the (schematic) approximate Jones-Nelson curve. The data point at U_{max} and a point at a slightly lower energy are used to determine B and C in Eq. (1). The point at $U=0$, corresponding to the origin of the stress-strain curve, is used to determine A. Alternatively, the values of A, B, and C can be determined from a least-squares error fit of all of the data points as described in the Appendix. The approximate Jones-Nelson curve is an accurate interpolation of the actual data for strain energies between zero and U_{max} (even more so than is deduced from examination of the schematic, exaggerated representation in Fig. 3). In addition, the approximate curve has the same shape as the actual curve in the neighborhood of U_{max} and is a plausible extension of the actual data for strain energies greater than U_{max}.

However, the use of the Jones-Nelson equation, Eq. (1), as an extrapolation of uniaxial data is restricted. At some large value of strain energy, designated as $\bar{U}$, the approximate mechanical property curve in Fig. 3 crosses the U axis (i.e., the extrapolated value of the mechanical property becomes negative). If a mechanical property is less than or equal to zero, a thermodynamic constraint on the mechanical property of a material is violated. This constraint, imposed on the properties to avoid the creation of energy, is that the work done by the stresses applied to a material must be positive. Lempriere[14] interprets this constraint as meaning that both the stiffness and compliance matrices of an orthotropic material must be positive definite. These matrices are positive definite only if the mechanical properties E_1, E_2, and G_{12} are positive (in addition to some other relations being necessary between all the material properties). From a practical standpoint, a zero modulus leads to a zero on the main diagonal of the stiffness matrix which cannot be inverted subsequently in a finite element computer program. Thus, the mechanical properties of a material cannot be defined with Eq. (1) for strain energies greater than or equal to $\bar{U}$.

The specific value of strain energy at which the mechanical property becomes negative is, by inspection of Eq. (1),

$$\bar{U}=B^{-1/C} \tag{3}$$

if U_0 is one unit of energy (e.g., 1 psi). Recall that B is the initial curvature and C is the rate of change of curvature of a stress-strain curve. Thus, $\bar{U}$ is largest for stress-strain curves with low initial curvature and low rate of change of curvature. Accordingly, the Jones-Nelson model can be used for large values of energy only when the stress-strain curves have slight nonlinearities. Conversely, the Jones-Nelson model is not expected to be applicable for materials with strong stress-strain curve nonlinearities without some modification.

To be valid, the stress-strain behavior implied from Eq. (1) must be a reasonable extension of the actual stress-strain behavior of the material. We can show that, in the typical implied stress-strain curve, the stress reaches a maximum value and then decreases as the strains increase as in Fig. 4. Also, the strain energies determined from the implied stress-strain curves approach but never reach the value $\bar{U}$, i.e.,

$$\lim_{\substack{\sigma\to 0\\ \epsilon\to\infty}} U=\bar{U}=B^{-1/C} \tag{4}$$

However, this stress-strain behavior in Fig. 4 is not representative of fiber-reinforced composite materials over the entire energy range $0<U<\bar{U}$. The schematic stress-strain curve reaches a maximum stress at the point $(\tilde{\sigma},\tilde{\epsilon})$ and is representative of fiber-reinforced composite materials for the energy range $0<U<\tilde{U}$ (where $\tilde{U}=\tilde{\sigma}\tilde{\epsilon}/2$). However, the implied stress-strain behavior to the right of $(\tilde{\sigma},\tilde{\epsilon})$ is not observed for fiber-reinforced composite materials. Thus, the basic Jones-Nelson material model cannot be used as an extrapolation for energies as large as $\bar{U}$ but must be restricted to energies less than or equal to $\tilde{U}$. This range is not sufficient to treat practical problems, and so modifications of the model are essential.

Extended Stress-Strain Curve Approach

We could extend the mechanical property vs energy behavior directly but feel that a discussion based on the extension of the stress-strain behavior is understood more easily. We shall subsequently examine the implications of the stress-strain curve extensions for the mechanical property vs energy curves. Basically, we could describe the problem to be avoided as a decreasing stress-strain curve as in the right side of Fig. 4. Thus, we make sure the stress-strain curve never decreases. In fact, we generally have a rising stress-strain curve as in Fig. 5. There, we fit the Jones-Nelson model to the input data points (actually, we fit the Jones-Nelson model to the corresponding points on the mechanical property vs energy plot) over their defined range. Beyond that range, the stress-strain curve must be extrapolated under multiaxial stress conditions. Three simple possibilities exist for the nature of the continuation of the stress-strain curve. First, the curve could become horizontal and remain horizontal (the lower bound on the possible behavior). Second, the curve could continue with the slope at the last data point (the upper bound on the possible behavior). Third, the curve could continue with a slope intermediate to that in cases 1 and 2. Of course, the curve could continue to be nonlinear, but we have no information as to its shape, and so we approximate it with a straight line as the first order and hence simplest approximation of the actual behavior. Any extrapolation beyond known behavior is somewhat arbitrary. Our objective

is to extend the behavior in a plausible and simple fashion hopefully to represent the real multiaxial behavior. We shall subsequently evaluate the work of our approach by comparing our predicted strain response with measured strain response under multiaxial stress conditions. First, however, we describe the extrapolation further.

Specifically, we extrapolate the implied stress-strain curve until a desired slope (tangent modulus to the stress-strain curve) is reached. After that slope is reached, we define the stress-strain curve to have that slope for all higher stresses and strains. A schematic mechanical property vs energy curve corresponding to the extended stress-strain curve is shown in Fig. 6. There, the extended mechanical property curve departs from the Jones-Nelson curve at the transition point and approaches asymptotically the tangent modulus $(d\sigma/d\epsilon)^*$ of the extrapolated stress-strain curve (while the Jones-Nelson curve decreases to zero at $\bar{U}$). Thus, the mechanical property can never be zero as long as the tangent modulus is not zero (i.e., as long as the extrapolated stress-strain curve is not horizontal in Fig. 5).

This overall extended stress-strain curve approach degenerates to the several subapproaches already mentioned. First, if the tangent modulus $(d\sigma/d\epsilon)^*$ in Fig. 6 were zero, the extrapolated stress-strain curve would be horizontal. This situation could occur with an implied $\sigma_0=\sigma^*$ $(=\bar{\sigma})$ in Fig. 5. Alternatively, a value of $\sigma_0=\sigma^*$ could be prescribed whereupon the implied stress-strain curve would not fit the data quite as well as implied in Fig. 5. A second subapproach, or model, is to use the slope at the last data point in Fig. 5 as the slope of the extrapolated stress-strain curve. However, real nonlinear stress-strain curves probably have a slope less than that at the last data point. A third subapproach is that the stress-strain curve can be forced to connect to a fixed line on a stress-strain plot as opposed to a fixed slope. That is, we ask that the stress-strain curve be connected to a straight line with equation $\sigma=m\epsilon+\sigma_0$ instead of merely specifying the slope m. This approach is useful in fitting the stress-strain curves while simultaneously considering the statistical nature of failure data which can be described with such a line.[15] A disadvantage of this approach is that the fit of the actual stress-strain data is not as good as with other approaches.

The foregoing extended stress-strain curve approaches are useful in modeling many types of materials. Examples of modeling boron/epoxy and graphite/epoxy fiber-reinforced composite materials are shown in the next section.

Uniaxial Off-Axis Loading Results

We first briefly describe the theory involved in uniaxial loading of a lamina in nonprincipal material directions. Then, we present our predicted strains under that loading for boron/epoxy and graphite/epoxy laminae. Moreover, we compare our predicted strains to those of Hahn and Tsai[8] and also to the measured strains of Cole and Pipes.[2] The results presented are but a sample of the kind of work necessary to obtain such strain predictions and correlations.

Theory of Uniaxial Off-Axis Loading

The nonconstant mechanical properties of a nonlinear material are determined easily from Eq. (1) if the strain energy is known. However, the value of U is not known because the stresses, strains, and mechanical properties are highly interdependent. The stresses and strains must be used to determine the strain energy, which, in turn, is used to determine the mechanical properties. Simultaneously, the mechanical properties must be used to determine the stresses and strains. Thus, stress analysis of materials with nonlinear stress-strain behavior is quite complex. Nonlinear stress-strain problems are even difficult to solve by direct substitution of Eq. (1) in the stress-strain relations. This complexity of the direct substitution procedure is discussed in this section for a simple uniaxial loading problem. Then, a more general and more practical iteration technique that can be extended readily to even more complicated problems is described.

We want to predict the strains in a lamina under uniaxial loading $\sigma_x=\sigma$, $\sigma_y=\tau_{xy}=0$ at some angle θ to the fiber (1) direction. These strains are related to the applied stress through

$$\epsilon_x=\bar{S}_{11}\sigma, \quad \epsilon_y=\bar{S}_{12}\sigma, \quad \gamma_{xy}=\bar{S}_{16}\sigma \tag{5}$$

where the $\bar{S}_{ij}$ are the usual transformed compliances[1] which depend on the strain energy, $U=\sigma\epsilon_x/2$. Thus, the governing equations are transcendental since the strains in essence depend on themselves. In what follows, we restrict our attention to the simple problem of a material with a single shear nonlinearity so that we can compare our approach with that of Hahn and Tsai.[8]

Two methods of solution are possible for this problem. First, we could use a direct method in which the strain ϵ_x is expressed in terms of the energy and the parameters in the mechanical property vs strain energy equation, Eq. (1), for $G_{12_{sec}}$ by substitution of the transformation relations for the compliance $\bar{S}_{11}$. The resulting nonlinear equation in ϵ_x is

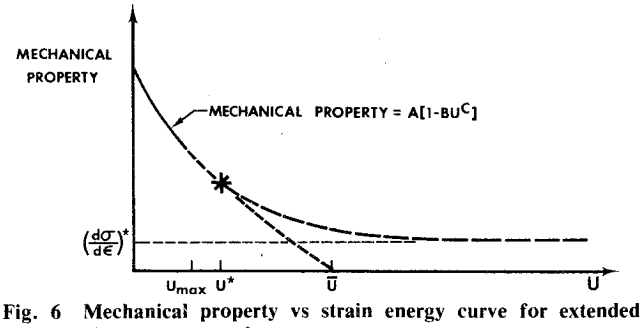

Fig. 6 Mechanical property vs strain energy curve for extended stress-strain curve approach.

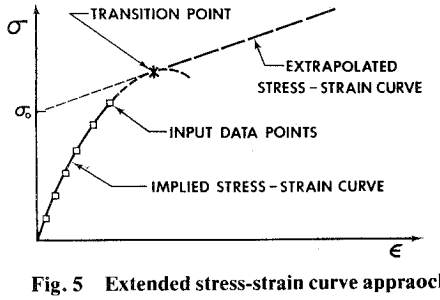

Fig. 5 Extended stress-strain curve appraoch.

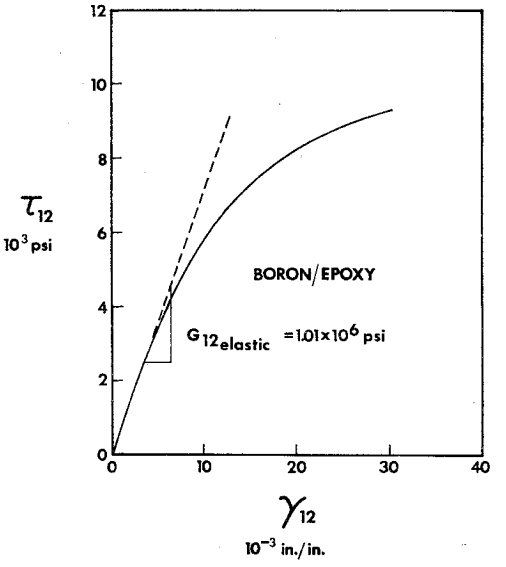

Fig. 7 Shear stress - shear strain behavior for boron/epoxy.

solved readily by several numerical methods (e.g., interval halving, Newton-Raphson, etc.). This direct approach is much more complicated than that of Hahn and Tsai,[8] who obtain an explicit relation for ϵ_x in terms of the loading and known material parameters including the nonlinear shear term. However, this complexity is the price we pay for the capability of having more than one nonlinearity in the material properties. The direct method is even more involved when more than one nonlinearity is included because the nonlinear equation is more complicated. Moreover, under multiaxial loading, the number of such complicated equations is equal to the number of loads applied (e.g., three for σ_x, σ_y, and τ_{xy}).

Accordingly, we choose the iteration technique which is displayed in Fig. 7 of Ref. 10 for all general loading problems. At each iteration of the nonlinear procedure, we analyze a linear elastic system with properties determined from the strain energy of the preceding iteration (use elastic properties to start the procedure). At convergence, the final linear elastic system is equivalent to the secant moduli of the nonlinear elastic body. This iteration technique is the same irrespective of the number of material property nonlinearities or the number of loadings. Moreover, the iteration technique is adapted more easily to laminate stress analysis problems where the direct method would have $3N$ coupled nonlinear equations for an N-layered laminate under arbitrary load. The coupled nonlinear equations are very awkward to obtain, and also the solution of that many equations is not practical when the simpler alternative of the iteration approach is well developed. Finally, the iteration technique is also well suited to finite element formulations, whereas the direct solution technique is utterly hopeless.

Boron/Epoxy Lamina Results

We note first from the Cole and Pipes data[2] that boron/epoxy (NARMCO 5505) has significantly nonlinear shear behavior, as shown in Fig. 7. The curve for E_2 is slightly nonlinear, but we shall regard it as linear. The curves for E_1 and ν_{12} are linear. Thus, the constant properties are

$$E_1 = 30.1 \times 10^6 \text{ psi}, \quad E_2 = 2.87 \times 10^6 \text{ psi}, \quad \nu_{12} = 0.225 \qquad (6)$$

We develop the material model by fitting the Jones-Nelson model, and the present variation thereof, to the $G_{12_{sec}}$ vs energy curve in Fig. 8 using the nonlinear regression analysis described in the Appendix. Note in Table 1, where the values of A, B, and C thereby obtained are reported, that $A = 1.01 \times 10^6$ psi is higher than Hahn and Tsai's G_{12} of 0.8×10^6 psi. That is, the actual initial tangent modulus is much higher for nonlinear stress-strain curves than most people would determine by placing a straightedge on the curve and reading an intercept. We draw these conclusions from our experience with many computer-generated plots of stress-strain curves in tandem with their associated mechanical property vs energy curves. We now proceed to predict strains under uniaxial loading at 15, 30, and 60 deg to the fiber direction.

15-deg Off-Axis Results

Strains are measured by Cole and Pipes[2] for stresses up to 36,000 psi for which the strain energy is 147 psi. Since the shear behavior is known only up to an energy of 139 psi, an extrapolation is necessary. We choose to extend the slope from the last data point for which the slope is 0.048×10^6 psi. This approach with $A = 1.01 \times 10^6$ psi and the corresponding values of B and C given in Table 1 is used to obtain Fig. 9. There, the Cole and Pipes data are shown along with the Hahn and Tsai predictions [$S_{66} = 1.25 \times 10^{-6}$ (psi)$^{-1}$ and $S_{6666} = 1.53 \times 10^{-14}$ (psi)$^{-3}$] which are always less than the measured strains. The present predictions are also less than the measured strains but are more accurate than the Hahn and Tsai predictions for stresses less than 35,000 psi. Above 35,000 psi, the present strains are as much as 15% too high, whereas below that stress the present strains are at most 10% too low. Thus, our results have too much curvature at high stress levels.

Table 1 Boron/epoxy lamina strain predictions for 15-deg off-axis loading ($E_1 = 30.1 \times 10^6$ psi, $E_2 = 2.87 \times 10^6$ psi, $\nu_{12} = 0.225$)

	ϵ_x, 10^{-3} in./in.			
			Present theory $A = 1{,}010{,}000$ psi, $B = 0.1622$, $C = 0.2942$	
σ_x, 10^3 psi	Cole and Pipes (measured)	Hahn and Tsai (predicted[a])	Extended $G_{12} - U$ curve	Extended $\tau - \gamma$ curve[b]
4	0.50	0.435	0.410	0.410
8	1.00	0.892	0.884	0.884
12	1.59	1.395	1.423	1.423
16	2.28	1.968	2.042	2.042
20	3.13	2.632	2.765	2.765
24	4.13	3.410	3.636	3.636
28	5.38	4.327	4.741	4.741
32	6.75	5.404	6.300	6.300
36	8.23	6.665	9.532	9.189

[a] $S_{66} = 1.25 \times 10^{-6}$ (psi)$^{-1}$ and $S_{666} = 1.53 \times 10^{-14}$ (psi)$^{-3}$.
[b] Slope = 62,466 psi.

We examine another approach to predicting the 15-deg off-axis strains in Table 1. There, the results just discussed are in the last column, the measured values are in column 2, and the Hahn and Tsai predictions are in column 3. If we simply extend the basic G_{12}-U curve, then an overly large strain is predicted at 36,000 psi because the hump of the τ-γ curve is being approached. Note that the strain predictions for the various extension approaches in the last two columns of Table 1 are identical for stresses up to 32,000 psi. This situation occurs because those approaches are indeed identical up to the point where an extrapolation is made.

We would expect better results than what we obtained for such a good fit of the G_{12}-U curve in Fig. 8. One immediate reaction is that ignoring the E_2 nonlinearity adversely affects the results. However, including that nonlinearity leads to negligible changes in the strain predictions (only the fifth significant figure changes). We next observe that the measured shear data are not consistent. In fact, if we back-calculate G_{12} from the initial slope E_x of each of the off-axis tests by use of the usual elastic transformations for $\bar{S}_{11}$ and Eq. (6), we find $G_{12} \times 10^{-6}$ (psi)$^{-1} = 0.655$ for $\theta = 15$ deg, 0.843 for $\theta = 30$ deg, 0.871 for $\theta = 45$ deg, 0.795 for $\theta = 60$ deg, and 0.662 for $\theta = 75$ deg. These discrepancies are not due to shear coupling[16] because the test specimens are too long for such an influence to exist. (The maximum predicted error due to shear coupling is 4% and occurs at $\theta = 15$ deg; the errors for

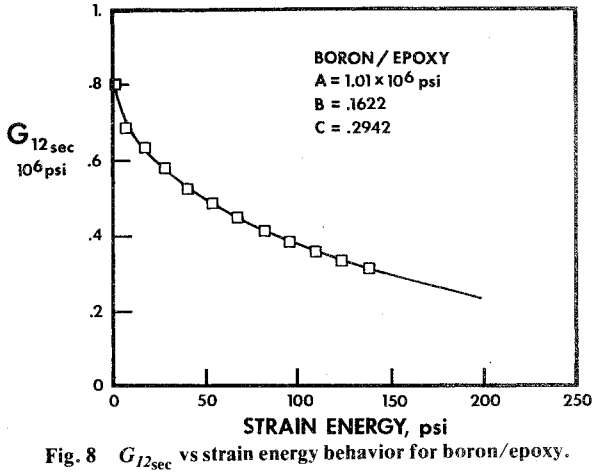

Fig. 8 $G_{12_{sec}}$ vs strain energy behavior for boron/epoxy.

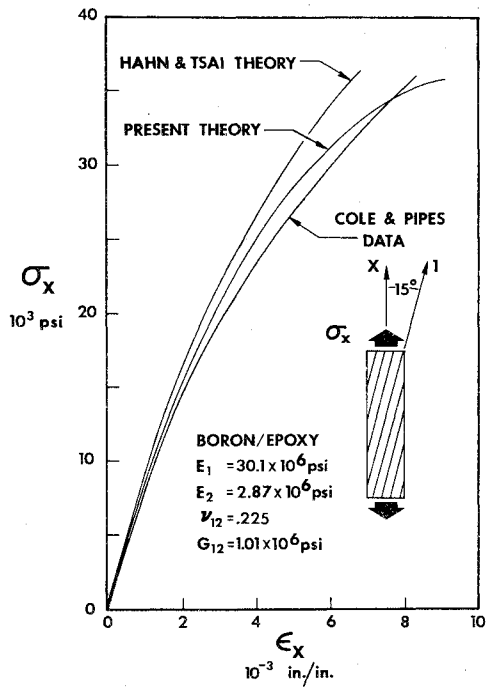

Fig. 9 15-deg off-axis stress-strain behavior for boron/epoxy.

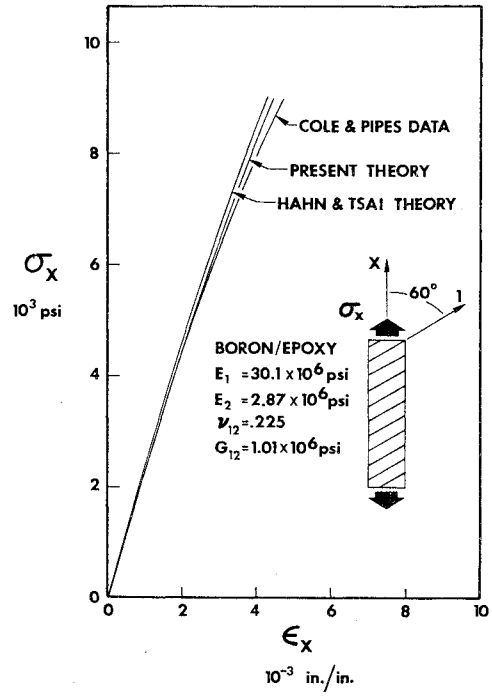

Fig. 11 60-deg off-axis stress-strain behavior for boron/epoxy.

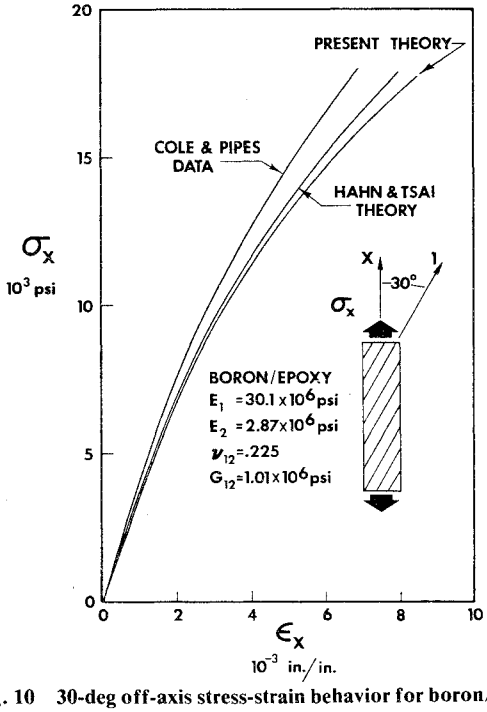

Fig. 10 30-deg off-axis stress-strain behavior for boron/epoxy.

the other off-axis angles are 1% or less.) Instead, the most plausible explanation may be that the specimens effectively have different properties because they were loaded at different times in the life of the material. Shear response data can be highly dependent on factors such as the cure cycle. In view of this apparent aging effect, we cannot expect to obtain any better correlation of the data than we obtained.

30-Deg Off-Axis Results

For 30-deg and higher off-axis tests, the strain energy is always lower than $U_{max} = 139$ psi for the shear data. Thus, no extrapolations of the stress-strain curves or G_{12}-U curves are necessary. The present results in Fig. 10 are obtained with the values of A, B, and C in Table 1. Our strains are overpredictions of the measured strains at all stress levels reaching a maximum error of 27% at 18,000 psi. Hahn and Tsai's results are 19% too high at that stress.

60-Deg Off-Axis Results

For 60-deg off-axis loading, our strain predictions in Fig. 11 are closer to Cole and Pipes' data than are Hahn and Tsai's predictions.

Other Results

Results for 45-deg off-axis loading are qualitatively similar to the 30-deg results in Fig. 10. Moreover, 75-deg results are essentially comparable to the 60-deg results in Fig. 11.

In summary, we obtain strain predictions that are quite comparable to the Hahn and Tsai predictions which are generally accepted. However, we use a material model with an inherent capability of treating all nonlinear material behavior. Thus, our model is more widely applicable than the Hahn and Tsai model.

Graphite/Epoxy Lamina Results

The stress-strain behavior of graphite/epoxy (4617/Modmor II) is similar to the behavior of boron/epoxy in that only the shear stress - shear strain curve is nonlinear. The other mechanical properties are

$$E_1 = 25.4 \times 10^6 \text{ psi}, \quad E_2 = 1.25 \times 10^6 \text{ psi}, \quad \nu_{12} = 0.46 \qquad (7)$$

We find $A = 0.9048 \times 10^6$ psi, $B = 0.0000741$, and $C = 1.705$ with nonlinear regression analysis. In contrast, Hahn and Tsai use an initial slope of 0.975×10^6 psi with $S_{66} = 0.1026 \times 10^{-5}$ (psi)$^{-1}$ and $S_{6666} = 2.363 \times 10^{-15}$ (psi)$^{-3}$.

15-Deg Off-Axis Results

The present strain predictions are better than the Hahn and Tsai predictions for high stress levels in Fig. 12 but are not as high as the Cole and Pipes data. However, over a substantial portion of the data, all three results are the same.

45-Deg Off-Axis Results

The present strain predictions are identical with the Hahn and Tsai predictions over the entire range of measured

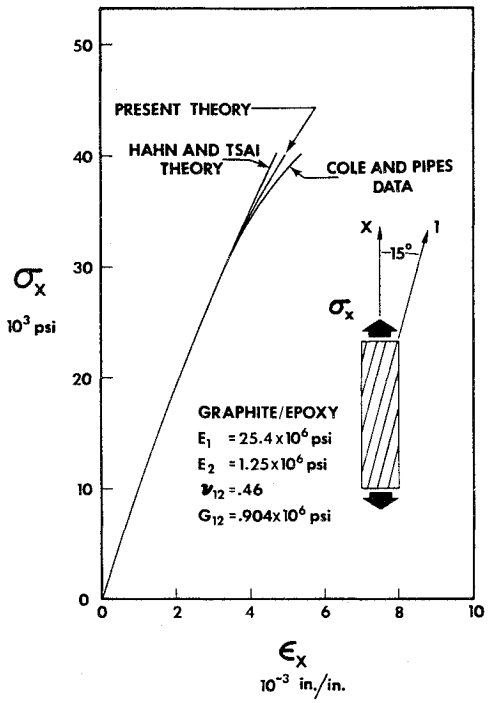

Fig. 12 15-deg off-axis stress-strain behavior for graphite/epoxy.

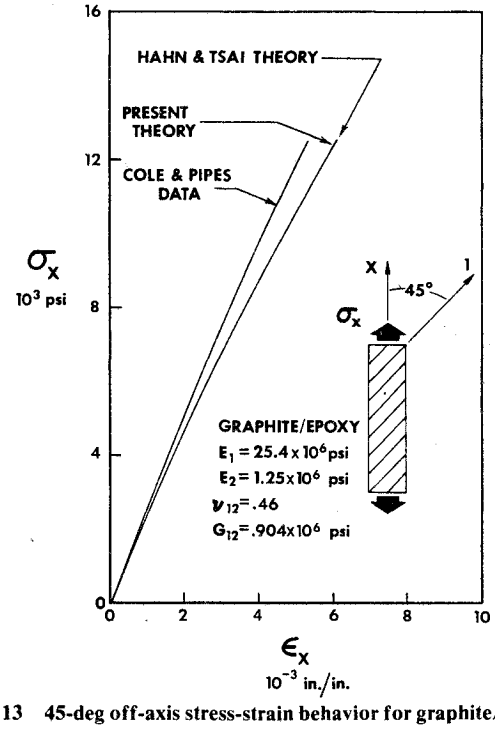

Fig. 13 45-deg off-axis stress-strain behavior for graphite/epoxy.

response in Fig. 13. There, both theories led to overprediction of the strain behavior. The foregoing results for graphite/epoxy are a reinforcement of the hypothesis that the present theory leads to results essentially the same as those obtained with the Hahn and Tsai model. However, the present theory is applicable to more than one nonlinearity.

Concluding Remarks

Significant extensions of the Jones-Nelson material model for nonlinear stress-strain behavior of orthotropic materials are described. The key elements of the new models include treatment of more pronounced nonlinearities and more highly orthotropic behavior than for the original model which was developed for mildly nonlinear, slightly orthotropic graphitic materials.[10-13] These new elements of the model are needed to represent the behavior of fiber-reinforced composite materials. These nonlinearities are increased orthotropy lead to a requirement of extending the Jones and Nelson model to substantially larger values of strain energy than measured in uniaxial materials characterization tests. Several methods of performing the extrapolation are compared.

Strains are predicted with the new models for uniaxial loading of boron/epoxy and graphite/epoxy laminae in nonprincipal material directions. Specific evaluation of our predicted strains is hampered by inconsistencies in the measured off-axis response. These inconsistencies are believed to be caused by the various test specimens being loaded at different ages of the material. This aging effect apparently overshadows our efforts to obtain precise correlation of our predictions with the measured strains. However, our predicted strains agree with strains measured by Cole and Pipes[2] about as well as those of previous theories. For example, our strains are sometimes in better agreement with and sometimes in worse agreement with the measured strains than Hahn and Tsai's predictions.[8] Thus, with this agreement for a limited class of problems (i.e., a single shear nonlinearity), we propose our model for use with fiber-reinforced composite materials with more than one nonlinearity. That is, we have a more broadly applicable model than previous theories since we can treat materials such as boron/aluminum and carbon/carbon which have multiple mechanical property nonlinearities.

Appendix: Determination of A, B, and C by Nonlinear Regression Analysis

We have a finite set of points in the mechanical property vs energy plane (Fig. 3) which we want to approximate with a curve of the form in Eq. (1). We want to make the approximation in the least-squares error sense. That is, we calculate A, B, and C (after U_0 is specified) so that the curve passes through the data such that the sum of the squares of the vertical differences between the curve and the various data points is minimized.

The Jones-Nelson nonlinear material model equation, Eq. (1), is not directly amenable to a least-squares error fit because the equation is not that of a straight line. However, we rearrange the equation in the form

$$1-\text{mechanical property}_i/A_i = B_i(U/U_0)^{C_i} \tag{A1}$$

take the natural logarithm of both sides of the equation,

$$\ell n(1-\text{mechanical property}_i/A_i) = \ell nB_i + C_i(\ell nU - \ell nU_0) \tag{A2}$$

and further stipulate that $U_0 = 1$ psi so that

$$\ell n(1-\text{mechanical property}_i/A_i) = \ell nB_i + C_i \ell nU \tag{A3}$$

Note that Eq. (A3) is of the form

$$y = a_0 + a_1 x \tag{A4}$$

which is the equation of a straight line. That is, we have performed a linearizing transformation.[17] Thus, we can now apply a least-squares fit of the transformed variables in the foregoing form, where

$$y = \ell n(1-\text{mechanical property}_i/A_i) \tag{A5a}$$

$$a_0 = \ell nB_i, \quad a_i = C_i, \quad x = \ell nU \tag{A5b}$$

The values of a_0 and a_1 for a least-squares fit to the linearized equations are[17]

$$a_0 = \frac{\Sigma y \Sigma(x^2) - \Sigma x \Sigma(xy)}{n\Sigma(x^2) - (\Sigma x)^2}, \quad a_1 = \frac{n\Sigma(xy) - (\Sigma x)(\Sigma y)}{n\Sigma(x^2) - (\Sigma x)^2} \tag{A6}$$

where n is the number of data points and

$$\Sigma x = \sum_{i=1}^{n} x_i, \quad \Sigma(x^2) = \sum_{i=1}^{n} (x_i)^2, \quad (\Sigma x)^2 = \left(\sum_{i=1}^{n} x_i \right)^2 \tag{A7a}$$

$$\Sigma y = \sum_{i=1}^{n} y_i, \quad \Sigma(xy) = \sum_{i=1}^{n} x_i y_i \tag{A7b}$$

Then, we obtain B_i and C_i by inverting the transformation:

$$B_i = \ell n^{-1} a_0, \quad C_i = a_1 \tag{A8}$$

However, we have not yet determined the value of A_i corresponding to a least-squares error fit. Actually, we have obtained only a least-squares fit of B_i and C_i for a *specified* value of A_i.

To determine A_i, we must minimize the squares of the errors

$$e_j^2 = \sum_{i=1}^{n} [\overline{M.P.}_j(U_i) - M.P._j(U_i)]^2 \tag{A9}$$

where $\overline{M.P.}_j$ is the jth mechanical property from the actual data at the n data points, and $M.P._j$ is the jth mechanical property from the Jones-Nelson equation, Eq. (1). We do not perform this minimization by finding where the derivative of the error squared is zero. Instead, we use a brute force, but effective, technique of keeping track of the error for various values of A_i and searching to find the value of A_i for which the error is smallest. That is, we increase A_i in increments from its smallest possible value of the secant modulus to the first data point until the error, which first decreases, begins to increase. Then, we successively halve the increment size and search the region around the minimum until we have defined the value of A_i to a desired level of accuracy.

The foregoing procedure must be modified slightly for Poisson's ratios (or moduli) which increase with increasing energy. Then, y in Eq. (A3) must be redefined as

$$y = \ell n(\text{mechanical property}_i / A_i - 1) \tag{A10}$$

in order to have a value for the logarithm. Moreover, B_i is then $-\ell n^{-1} a_0$ in Eq. (A8). Finally, A_i in the foregoing search procedure is decreased in increments until the minimum error is reached.

The results obtained with the foregoing regression analysis are very satisfactory for Young's moduli and range from satisfactory to not very good for Poisson's ratios. The problem with the Poisson's ratios is that the initial value (A_i) is often too high to be realistic (0.67 as opposed to a three-point fit value of 0.12 for $\nu_{r\theta}$ of ATJ-S graphite). Thus, a three-point fit as described in Refs. 10-13 may be desirable for some Poisson's ratios. Overall, the material modeling procedure is hastened drastically with the regression approach. That is, the values of A, B, and C for a good fit (presumably the best fit) are obtained with a single computer run as opposed to the many runs necessary to find the best three-point fit.

Acknowledgment

This research was sponsored by the Air Force Office of Scientific Research/NA (Grant 73-2532).

References

[1] Jones, R. M., *Mechanics of Composite Materials*, McGraw-Hill, New York, 1975.

[2] Cole, B. W. and Pipes, R. B., "Filamentary Composite Laminates Subjected to Biaxial Stress Fields," IIT Research Inst., Chicago, Ill. and Drexel University, Philadelphia, Pa., Air Force Flight Dynamics Lab.Technical Report AFFDL-TR-73-115, June 1973.

[3] Ramsey, J. E., Waszczak, J. P., and Klouman, F. L., "An Investigation of the Nonlinear Response of Metal-Matrix Composite Laminates," AIAA Paper 75-787, 16th AIAA/ASME/SAE Structures, Structural Dynamics, and Materials Conference, Denver, Colo., May 27-29, 1975.

[4] Starrett, H. S., Weiler, F. C., and Pears, C. D., "Thermostructural Response of Carbon-Carbon Materials under High Heat Flux Environments," Southern Research Inst., Birmingham, Ala., Air Force Materials, Lab. Technical Report AFML-TR-74-232, June 1975.

[5] Whitney, J. M., *Air Force Workshop on Durability Characteristics of Resin Matrix Composites*, Columbus, Ohio, Sept. 30-Oct. 2, 1975.

[6] Petit, P. H. and Waddoups, M. E., "A Method of Predicting the Nonlinear Behavior of Laminated Composites," *Journal of Composite Materials*, Vol. 3, Jan. 1969, pp. 2-19.

[7] Hashin, Z., Bagchi, D., and Rosen, B. W., "Non-Linear Behavior of Fiber Composite Laminates," Materials Sciences Corp., Blue Bell, Pa., NASA CR-2313, April 1974.

[8] Hahn, H. T. and Tsai, S. W., "Nonlinear Elastic Behavior of Undirectional Composite Laminae," *Journal of Composite Materials*, Vol. 7, Jan. 1973, pp. 102-118.

[9] Sandhu, R. S., "Nonlinear Response of Unidirectional and Angle-Ply Laminates," *Journal of Aircraft*, Vol. 13, Feb. 1976, pp. 104-111.

[10] Jones, R. M. and Nelson, D. A. R., Jr., "A New Material Model for the Nonlinear Biaxial Behavior of ATJ-S Graphite," *Journal of Composite Materials*, Vol. 9, Jan. 1975, pp. 10-27.

[11] Jones, R. M. and Nelson, D. A. R., Jr., "Further Characteristics of a Nonlinear Material Model for ATJ-S Graphite," *Journal of Composite Materials*, Vol. 9, July 1975, pp. 251-265.

[12] Jones, R. M. and Nelson, D. A. R., Jr., "Material Models for Nonlinear Deformation of Graphite," *AIAA Journal*, Vol. 15, June 1976, pp. 709-717.

[13] Jones, R. M. and Nelson, D. A. R., Jr., "Theoretical-Experimental Correlation of Material Models for Nonlinear Deformation of Graphite," *AIAA Journal*, Vol. 15, Oct. 1976, pp. 1427-1435.

[14] Lempriere, B. M., "Poisson's Ratio in Orthotropic Materials," *AIAA Journal*, Vol. 6, Nov. 1968, pp. 2226-2227.

[15] Crose, J. G., Prototype Development Associates, Santa Ana, Calif., personal communication, Jan. 1976.

[16] Pagano, N. J. and Halpin, J. C., "Influence of End Constraint in the Testing of Anisotropic Bodies," *Journal of Composite Materials*, Vol. 6, Jan. 1968, pp. 18-31.

[17] Lipson, C. and Sheth, N. J., *Statistical Design and Analysis of Engineering Experiments*, McGraw-Hill, New York, 1973, pp. 383, 401.